

High-Temperature Fatigue Test on P91 Induction Bent Pipe of PGSFR for Applicability Analysis

Tae-Won Na^{a*}, Jong-Bum Kim^a, Chang-Gyu Park^a, June Hyung Kim^a

^aKorea Atomic Energy Research Institute, Daedeok-daero 989-111, Yuseong-gu, Daejeon, Korea

*Corresponding Author : ntw@kaeri.re.kr

1. Introduction

Induction bending technology is expanding across industries such as coal and combined-fired power generation, shipbuilding, and offshore plants due to its ability to reduce welded joints, thereby enhancing structural integrity. However, applying it to nuclear safety-class pipes remains limited by strict nuclear standards. To address these limitation, recent studies have focused on exploring the applicability of induction bending [1-3]. This study evaluates the feasibility of applying induction bent P91 elbow pipes in the Prototype Gen-IV Sodium-cooled Fast Reactor (PGSFR) through high-cycle and low-cycle fatigue tests at high temperature to assess their structural integrity per ASME Code[4], confirming their suitability for safety-critical systems in advanced nuclear reactors.

2. High-Temperature Fatigue Tests of P91 Induction Bent Pipes

2.1 Fabrication of P91 Induction Bent Pipe Test Model

To facilitate the installation of an 8-inch P91 induction bent pipe into the structural test rig, two parallel flanges were welded to its end. Additionally, holes were machined at the opposite end, to accommodate the insertion of load pin from the test rig. Figure 1(a) and (b) show the fabricated test model and its schematic.

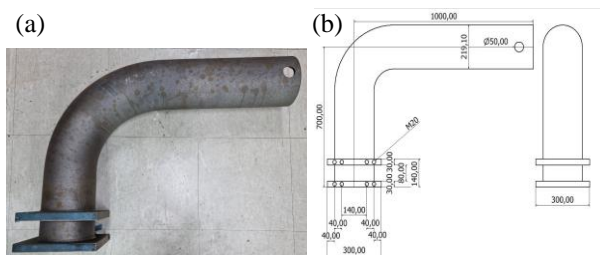


Figure 1. (a) Test model of the P91 induction bent pipe, (b) drawing of the test model

2.2 Test Equipment Setup

For the fatigue test of the test model, the structural test rig was set up as shown in Figure 2. This rig is capable of controlling a load up to 25 tons and a displacement of ± 100 mm. The operational unit includes a hydraulic actuator(Instron 8400), a load cell, and a LVDT, with signal processing handled by a DAQ system. An internal air circulation heater was specially fabricated for the elbow section of the test model to maintain a high-

temperature environment of approximately 550°C, ensuring a temperature variation within about 2%. This setup was designed to simulate the actual conditions of the piping being heated by flowing high-temperature sodium.

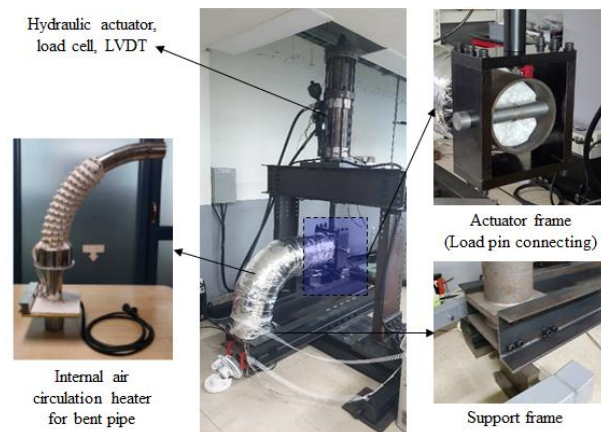


Figure 2. Structural test rig and internal air circulation heater

2.3 Fatigue Test Loadings

Material constants for the elastoplastic analysis model were derived from tensile and low-cycle fatigue tests previously conducted on specimens from the induction bent P91 pipe [3]. Detailed elastoplastic analyses of the test model were performed for various loads, and the results were used to determine the strain range at the neutral section of the elbow where maximum stress occurs. This strain ranges were then applied to the design fatigue curve of P91 at 550°C in ASME Code, Sec.III, Div.5[4] to evaluate the allowable cycles (fatigue life) as shown in Figure 3.

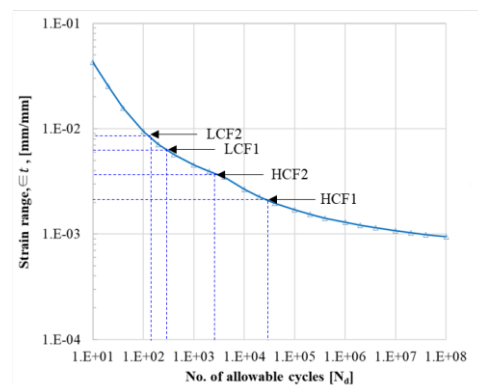


Figure 3. Design fatigue curve for P91 at 550°C in ASME Code and design fatigue life for cyclic loads

From this evaluation, two high-cycle and two low-cycle fatigue test loads were determined, respectively. The first and second rows in Table 1 and Figure 3 indicate the high-cycle fatigue test loads, while the third and fourth rows represent the low-cycle fatigue test loads. High-cycle fatigue test loads of ± 40 kN and ± 50 kN correspond to displacements of ± 12 mm and ± 15 mm, respectively, selected because these ranges exhibit mostly elastic behaviors. Displacements of ± 20 mm and ± 25 mm, which show elastoplastic behavior, were chosen as low-cycle fatigue test loads. A conservative margin of 30% was applied to the fatigue life for each load for fatigue test.

Table 1. Fatigue test loads and cycles

Test	Load	Max. strain range(ϵ_i) [mm/mm]	No. of allowable cycles[N_d]	No. of cycles with a 30% safety margin[N]
HCF1	± 40 kN	2.78E-03	8,674	11,277
HCF2	± 50 kN	3.81E-03	2,411	3,134
LCF1	± 20 mm	6.22E-03	302	393
LCF2	± 25 mm	8.76E-03	120	157

2.4 High-Cycle Fatigue Test

High-cycle fatigue tests were conducted at 550°C, applying cyclic loads of ± 40 kN(HCF1) and ± 50 kN (HCF2) vertically to the holes of the test model. HCF1 and HCF2 tests were carried out over 11,370 cycles (95 hours) and 3,152 cycles (35 hours), respectively. During the HCF1 test, the displacement amplitude at the load point increased from an initial 39.4mm to a final 46mm, an increase of 16.8%, as illustrated in Figure 4(a). In the HCF2 test, the displacement amplitude increased from an initial 41mm to a final 50mm, a 20% increase. Both HCF1 and HCF2 tests showed increases in displacement amplitude, indicative of the cyclic softening characteristics of P91 steel.

2.5 Low-Cycle Fatigue Test

Low-cycle fatigue tests were conducted at 550°C, applying cyclic displacement loads of ± 20 mm (LCF1) and ± 25 mm (LCF2) vertically to the holes of the test model. LCF1 and LCF2 tests were carried out for 413 cycles (6 hours) and 180 cycles (3.3 hours), respectively. The results of LCF1 showed that the reaction load history stabilized initially and then the load amplitude decreased from 135 kN to 131.9 kN, a 2.3% reduction, as shown in Figure 4(b). In LCF2, the load amplitude decreased from 154.2 kN to 151.9 kN, a reduction of 1.5%. These changes are characteristic of the cyclic softening characteristics of P91 steel.

2.6 Fatigue Damage Inspection

After the high-temperature fatigue tests, the test models were inspected for fatigue damage. The bending sections were cut to check for fatigue defects on the inner surfaces of the elbows where the highest stresses had been

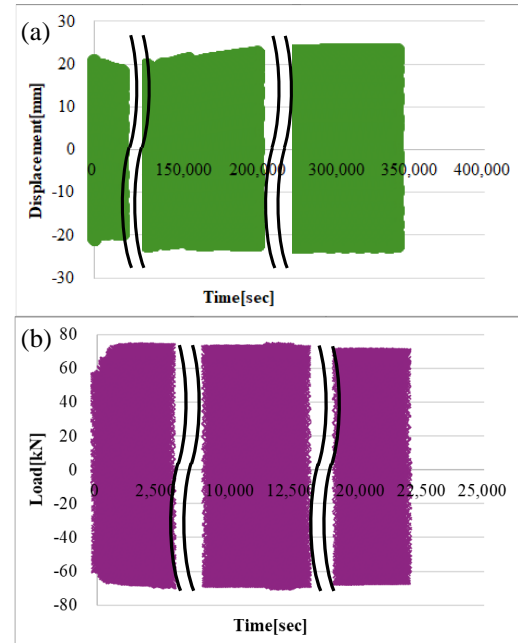


Figure 4. (a) Displacement amplitude change of HCF1 test, (b) Load amplitude change of LCF1 test

anticipated by elastoplastic analysis. This inspection was performed using fluorescent magnetic particle examination, which is highly effective for detecting surface defects as shown in Figure 5(a). The results revealed fine defects on the inner surfaces of the neutral section of all test specimens, distributed in a kidney shape along the axis of the piping, consistent with the stress concentration areas predicted by the stress distribution analysis as displayed in Figure 5(b). The orientation of these defects was also axial, matching the direction in which the highest circumferential stresses were expected to occur. No defects were found at other inspection sections on the inner and outer surfaces of the piping. Furthermore, to assess the severity of fatigue damage, specimens for Scanning Electron Microscopy(SEM) inspection were prepared from the elbows of each test model as shown in Figure 6(a). The inspection revealed that the maximum defect depth was 96.1 μ m, as illustrated in Figure 6(b). This defect depth is below the 3 mm crack length specified by the ASME Code, thus no cracks were considered to have occurred.

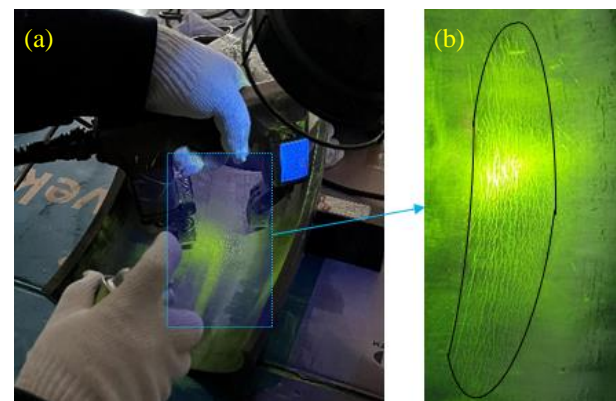


Figure 5. (a) Fluorescent magnetic particle inspection (b) detected defects

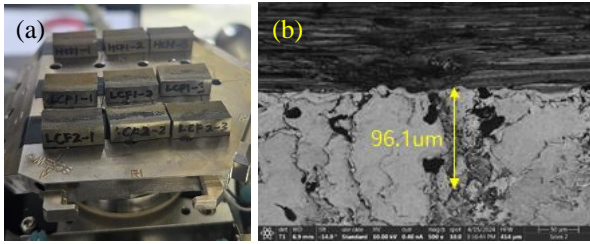


Figure 6. (a) SEM inspection specimens, (b) SEM image showing the maximum defect depth

3. Conclusion

Both high-cycle and low-cycle fatigue tests were performed on test models of P91 induction bent pipe. The tests confirmed that the maximum defect depth induced by fatigue loads was 96.1 μm , indicating that no cracks had developed based upon the ASME Code requirements. These high-temperature fatigue tests demonstrated that the induction bent P91 piping meets and exceeds the ASME Code's fatigue life requirements by a significant margin, and thus the structural integrity and applicability of induction bending technology under fatigue loading conditions had been validated. It affirms its potential for safety related pipe system in not only sodium-cooled fast reactor, but also other fourth-generation nuclear power plant.

Acknowledgement

This work was supported by a grant from the National Research Foundation of Korea (NRF) funded by the Korean government (Ministry of Science and ICT) (RS-2022-00155157).

REFERENCES

- [1] N.H. Kim, J.B. Kim, S.K. Kim, "Applicability of the induction bending process to the P91 pipe of the PGSFR", Nuclear Engineering and Technology 53, p1580-1586, 2021.
- [2] Tae-Won Na, Nak-Hyun Kim, Chang-Gyu Park, Jong-Bum Kim, and Il-Kwon Oh, "Validation of applicability of induction bending process to P91 piping of prototype Gen-IV Sodium-Cooled fast Reactor (PGSFR)", Nuclear Engineering and Technology 55, p3571-3580, 2023.
- [3] Tae-Won Na, Nak-Hyun Kim, Chang-Gyu Park, Junehyung Kim, Jong-Bum Kim and Il-Kwon Oh, "Applicability analysis of induction bending process to P91 piping of PGSFR by high-temperature fatigue test", Nuclear Engineering and Technology 56, p5190-5200, 2024.
- [4] ASME Boiler and Pressure Vessel Code, Section III, Division 5, High Temperature Reactors, 2021.